Fault-Tolerant Computing with Single Qudit Encoding

M. Mezzadri[†], ^{1, 2} A. Chiesa[†], ^{1, 2, 3} L. Lepori, ^{1, 2} and S. Carretta^{1, 2, 3, *}

¹ Università di Parma, Dipartimento di Scienze Matematiche, Fisiche e Informatiche, I-43124, Parma, Italy
² Gruppo Collegato di Parma, INFN-Sezione Milano-Bicocca, I-43124 Parma, Italy
³ UdR Parma, INSTM, I-43124 Parma, Italy

We present a general approach for the Fault Tolerant implementation of stabilizer codes with a logical qubit encoded into a single multi-level qudit, preventing the explosion of resources of multi-qubit codes. The proposed scheme allows for correction and universal quantum computation. We demonstrate its effectiveness by simulations on molecular spin qudits, finding an almost exponential suppression of logical errors with the qudit size. The resulting performance on a small qudit is remarkable when compared to qubit codes using thousands of units.

A "useful" quantum computer should be universal, accurate and scalable [1], i.e. capable to solve any kind of problem with an arbitrary small error and with resources which do not increase exponentially with the size of the problem or with the target error. Meeting these conditions on a noisy hardware requires a fault-tolerant (FT) quantum error correction (QEC) approach, which allows for universal quantum computation (QC) with an arbitrary error reduction, while remaining experimentally achievable. In practice, an elegant mathematical construction must be combined with a feasible physical implementation.

The standard way to tackle this problem relies on encoding the elementary unit of computation (a logical qubit, LQ) into a collection of distinct physical qubits [2–6]. In principle, this allows one to design QEC codes suppressing the error on the LQ compared to the elementary error probability (p) on each physical qubit, thus meeting FT for p below a certain threshold. Moreover, the error can be further reduced by a concatenated encoding, i.e. by increasing the number of physical qubits in the LQ [3, 7]. However, FTQC also demands a recipe to implement all the required gadgets (error correction, gates, measurements) without ever amplifying errors. This comes usually with an enormous cost in the number of physical qubits, required not only for the encoding, but also as ancillae for the various computational steps [7]. Different codes were developed along these lines, with increasingly higher threshold [8–17], but for all of them the most important road-block to an actual implementation remains the explosion in the number of physical qubits and gates for a reliable algorithm [13, 18, 19]. For instance, Fig. 1-(a) shows the circuit for a logical gate X_L followed by FT error correction (EC) using the five-qubit code [20], i.e. the smallest code correcting a generic one-qubit error. Even this compact encoding requires 25 qubits (5 to encode the logical state $|\bar{\psi}\rangle + 20$ ancillae) to achieve FTQC [10]. Moreover, to increase the correcting power (i.e. to tolerate more than a single error) a concatenation strategy is usually followed [Fig.1-(b)] [7], which recursively encodes a LQ into 5 lower-level units, thus quickly resulting in a dramatic increase of physical resources.

Here we pursue an alternative approach [Fig. 1-(c)] based on embedding a LQ into a *single* multi-level quantum system [21, 22] (a *qudit*), which is then corrected and operated in a FT manner. Along this line, cat and binomial codes in superconducting circuits and microwave modes [23, 24] or molecular spin systems [22, 25–27] have been recently proposed, reaching in some cases the break-even point and supporting "transparent" gates [28, 29] and error detection [30] with no error propagation [24, 31]. However, a FT implementation with error suppression to an arbitrary level must still be fully explored [24].

In our FT qudit approach (FTqd), an almost exponential error reduction comes only with a linear growth in the number of qudit levels, without increasing the complexity of the LQ with additional objects. This extremely simplifies the actual control of the hardware and could make the

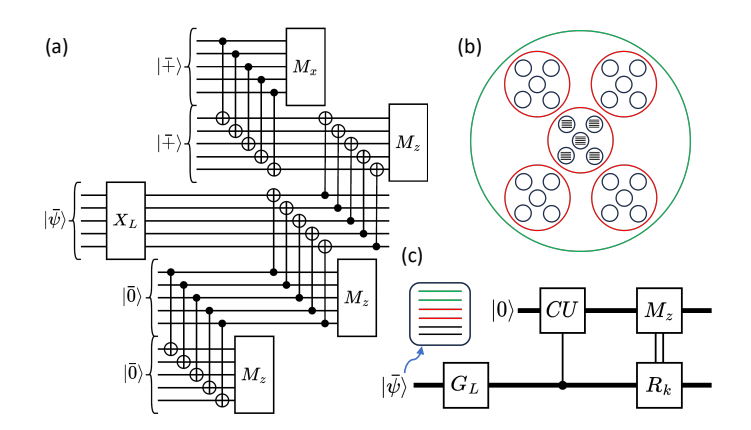


FIG. 1: Comparison between the FT circuit implementing a single-qubit logical gate and the consequent EC for (a) the five-qubit code with Steane EC and (c) our FTqd embedding a LQ into a single multi-level qudit (bold lines). The bar over $|\psi\rangle$ indicates this is an encoded logical state. While in (a) 25 qubits are needed to correct a single error and their number increases in a concatenated encoding (b), in (c) only 2 qudits suffice, with higher-order correction achieved by only adding a few levels.

FTqd a viable path towards the physical implementation of a "useful" quantum computing machine. We illustrate a stabilizer code allowing us to fault-tolerantly encode and process quantum information in a d-levels qudit. In particular, we show that errors can be detected and corrected by measuring stabilizer operators on a d/2-levels ancilla. Moreover, we show how to implement a universal set of logical single and two-qubit gates, only relying on the proper connectivity between the different eigenstates defining the LQ. As an example, we then present simulations on a platform based on molecular spin qudits [22, 26, 32], which allows for a hardware-efficient implementation of our scheme. Numerical simulations of all the QEC gadgets show that the logical error after correction propagates to higher orders than the physical error affecting the system (i.e. the error is suppressed to a larger extent). This demonstrates fault-tolerant QC. Moreover, we find logical errors decrease almost exponentially with the number of levels in the encoding.

General protocol – We first introduce the general mathematical framework of the stabilizer codes and then show which properties are needed on the hardware for their FT implementation.

Errors corrupting quantum information initially encoded in the pure state $\rho_0 = |\psi_0\rangle \langle \psi_0|$ are represented by Kraus operators E_k , i.e. the density matrix after possible errors is $\rho = \sum_k E_k \rho_0 E_k^{\dagger}$. Protection against a set of errors $\{E_k\}$ can be achieved by identifying code words $|0_L\rangle$ and $|1_L\rangle$ which satisfy Knill-Laflamme conditions [33]:

$$\langle 0_L | E_k^{\dagger} E_j | 0_L \rangle = \langle 1_L | E_k^{\dagger} E_j | 1_L \rangle$$
 (1a)

$$\langle 0_L | E_k^{\dagger} E_i | 1_L \rangle = 0. \tag{1b}$$

By using d dimensional qudits, at most d/2 different errors can be corrected. We then consider the vector set $\{|0_L\rangle, E_k|0_L\rangle, |1_L\rangle, E_k|1_L\rangle\}_{k=1}^{d/2}$, and the orthonormal basis set \mathcal{A} obtained from its Gram-Schmidt orthogonalization. We denote the set \mathcal{A} of error words as $\{|\ell, k\rangle\}$ with $\ell = 0, 1$ and $k = 0, \ldots, d/2$.

This choice highlights the basic idea to achieve FTQC, to perform logical operations independently of the error k [34]. Formally, given a gate G on a single qubit, the corresponding logical gate G_L that extends G to the protected LQ is given by $G_L \doteq G \otimes I_{d/2}$. This is equivalent to defining the logical Pauli operators:

$$X_L = \sum_{k=0}^{d/2-1} (|0,k\rangle \langle 1,k| + |1,k\rangle \langle 0,k|)$$
 (2a)

$$Z_L = \sum_{k=0}^{d/2-1} (|0,k\rangle \langle 0,k| - |1,k\rangle \langle 1,k|)$$
 (2b)

and $Y_L = -iZ_LX_L$. Then, a generic logical rotation about $\sigma = X, Y, Z$ is obtained $R_L^{\sigma}(\theta) = \exp[-i\sigma_L\theta/2]$. Two-qubit controlled logical gates CG can be realized in a similar way, by implementing CG independently of the error k on both the (logical) control and target (see SM). Finally, readout of the state of the LQ corresponds to a measurement of Z_L , which again translates into distinguishing the value of ℓ independently of the error k. Error detection translates into the stabilization of information through the measurement of

$$S = \sum_{k,\ell} \lambda_k |\ell, k\rangle \langle \ell, k| \tag{3}$$

where $\lambda_k \neq \lambda_{k'}$ for $k \neq k'$. This is the natural extension of standard stabilizers codes on qubits, with the important simplification that we have only one multi-valued stabilizer that gives directly the error syndrome instead of multiple two-valued stabilizers [35, 36]. Stabilization is achieved by exploiting a d/2-levels ancilla linked to the d-levels LQ and implementing a k-controlled operation CU [Fig. 1-(b)] between the logical qubit (control, initially in a generic state $|\bar{\psi}\rangle$ and the ancilla (target, initialized in its ground state $|0\rangle$). tion of the CU gate is defined as: $|\ell, k\rangle |0\rangle \mapsto |\ell, k\rangle |k\rangle$, $|\ell, k\rangle |k\rangle \mapsto -|\ell, k\rangle |0\rangle$ and the identity otherwise [37]. Therefore, CU maps each error k to a specific eigenstate of the ancilla. Hence, a final measurement of the ancilla in its eigenbasis $[M_z \text{ in Fig. } 1\text{-(b)}]$ identifies the error syndrome k and stabilizes information in the subspace $|\ell,k\rangle$. Here a single measurement for each LQ is sufficient, whereas in multi-qubit codes many measurements are needed for each syndrome, thus reducing the impact of measurement errors. The final recovery step R_k consists in mapping the stabilized $|\ell, k \neq 0\rangle$ into $|\ell, k = 0\rangle$.

Implementation – The actual FT implementation of the QC gadgets (EC, one- and two-qubit gates, readout) requires to perform them directly on encoded states, avoiding any decoding step [7]. We show this can be achieved by assuming a LQ encoded in a d-level quantum system in which transitions between any pair of levels can be induced by external stimuli (all-to-all connectivity).

As a prototypical example, we consider spin gudits encoded in Molecular Nanomagnets (MNMs), i.e clusters containing few interacting spins, whose spin Hamiltonian is usually well characterized and can be tailored to fit specific requirements [26, 38–42]. In particular, multispin molecules characterized by a proper pattern of antiferromagnetic competing exchange interactions display many low-energy multiplets with an all-to-all connectivity thanks to anisotropies [32, 43]. Hence, MNMs naturally provide a hardware-efficient implementation of the abstract concepts introduced above. In these systems (as in trapped ions [44, 45], atoms [46] and several other spin architectures [47, 48]) pure dephasing is by far the leading error (with decay time T_2), while spin relaxation at low temperature is orders of magnitude slower [49–51]. Therefore, we focus on pure dephasing.

Fig. 2 illustrates the implementation of representative single-qubit gadgets, focusing for simplicity on a

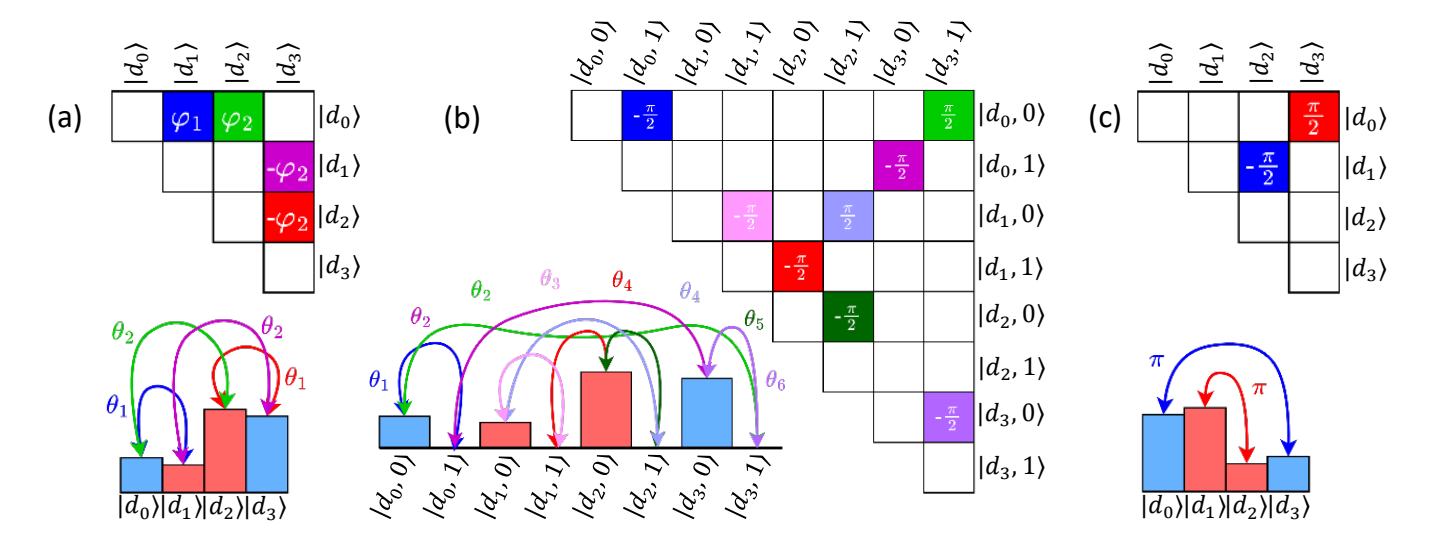


FIG. 2: Scheme of single-qubit gates (a), stabilization (b), and recovery (c) for a d=4 LQ, using the code words derived in Ref. [32]. In each panel the left histogram represents the populations of the eigenstates $(|d_j\rangle)$ assuming $\alpha=\beta=1/\sqrt{2}$, in blue (orange) for $\ell=0(1)$. The upper triangular matrix on the right is the driving Hamiltonian in the rotating frame, with filled boxes indicating the set of θ_i resonant pulses between pairs of eigenstates (arrows in the histograms) which are simultaneously sent to the system. Different colors of the arrows and boxes indicate different pulse frequencies, while phases are indicated on top. Eigenstates of the system qudit are indicated as $|d_j\rangle$, j=0,...,3. For stabilization (b) the eigenstates of a two-level ancilla (0,1) are also reported.

4-levels LQ. The extension to larger qudits is straightforward. Hereafter we use the error words derived in Ref. [32] for a molecular multi-spin cluster interacting with a nuclear spin bath which drives decoherence, because the specific choice does not qualitatively affect our conclusions. Let's start from a logical planar rotation $R_L^P(\theta,\phi) = \exp\left[-i\left(\cos\phi Y_L - \sin\phi X_L\right)\theta/2\right]$. From (2), we note that its realization requires resonant pulses between each eigenstate in the logical $\ell = 0$ subspace [blue bars in Fig. 2-(a)] and each one in the logical $\ell = 1$ subspace (orange bars). Different pulses of length θ_i are indicated by double arrows in the histogram and their phase φ_i is reported in the connectivity matrix H nearby. As detailed in the SM, one can show (with a generalized rotating frame formalism [52]) that the set of simultaneous pulses $\{\theta_i, \varphi_i\}$ implements the unitary $\exp \left|-i\tilde{H}\right|$, which corresponds to $R_L^P(\theta,\phi)$. Here we assume all the energy gaps to be spectroscopically distinguishable. Remarkably, since $\theta, \phi \in \mathbb{R}$, the resulting set of gates $R_L^P(\theta, \phi)$ is a universal set for a single logical qubit.

We now examine the stabilization process, reported in Fig. 2-(b). In this case, the eigenstates of both the LQ and of a d/2 levels ancilla are shown in the product basis $|d_j, k\rangle$. We recall that the ancilla is initialized in its ground state $|0\rangle$. CU stabilization requires to excite the ancilla iff the LQ is in k=1. This translates into the set of simultaneous pulses indicated in Fig. 2-(b) between each qudit eigenstate $|d_i\rangle$ with the ancilla in $|0\rangle$ and each qudit eigenstate $|d_j\rangle$ with the ancilla in $|1\rangle$. Following the

argument above, one can derive the connectivity matrix with pulse lengths and phases by taking the logarithm of CU (see SM). It is important to note that the ancilla does not need to be encoded. Indeed, it is excited to the eigenstate $|k\rangle$ with the same probability p_k of having an error E_k . Then, it suffers an error $E_{k'}$ with the conditional probability $p_k \, p_{k'}$ which therefore results to be of a higher order than the error on the qudit.

Fig. 2-(c) also shows the recovery step from k=1 to k=0, which is obtained by a pair of pulses within the two disjoint $\ell=0,1$ subspaces [53]. Other single-qubit gadgets (e.g., encoding) can be analogously obtained. Final k-independent readout of the LQ is accomplished by distinguishing orange and blue bars in the histograms of Fig. 2. Notice that fault-tolerance of all these operations is ensured by the all-to-all connectivity, which enables us to never decode the LQ and hence not to introduce additional errors.

Simulations – We now demonstrate the effectiveness of the single-qubit gadgets described above by numerical simulations in which we integrate the Lindblad equation for the system density matrix, subject both to pure dephasing and to the required sequence of pulses (see SM). In particular, we consider generic $R_L^P(\theta,\phi)$ rotations, followed by stabilization and correction and we report [Fig. 3-(a)] the final logical error $\bar{\mathcal{E}}_e$ as a function of the elementary error rate $1/T_2$. Here $\mathcal{E}_e = 1 - \mathcal{F}_e^2$, where \mathcal{F}_e is the entanglement fidelity [20] of the procedure [54], and we average on a universal set of (θ,ϕ) values. The

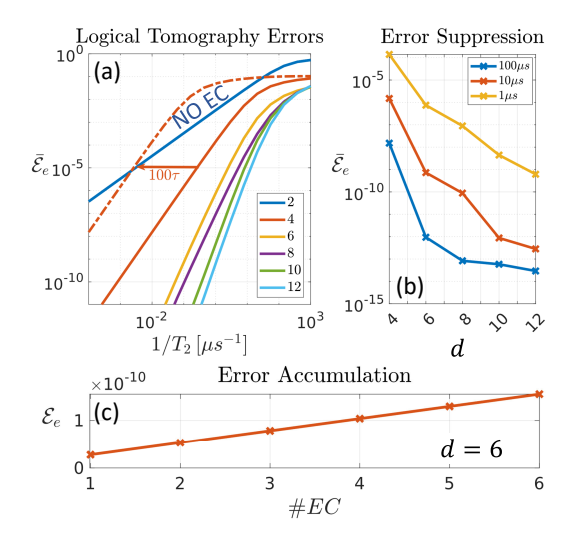


FIG. 3: Simulation of the FTqd implementation of single qubit logical gates on a MNM [32]. (a) Error $\mathcal{E}_e = 1 - \mathcal{F}_e^2$ as a function of $1/T_2$, where \mathcal{F}_e is the entanglement fidelity [20], averaged over different planar rotations $R_L^p(\theta,\varphi)$ for $(\theta,\phi) = (\frac{\pi}{4},\pi), (\frac{\pi}{2},\pi), (\frac{\pi}{2},-\frac{\pi}{2}), (\frac{\pi}{2},-\frac{\pi}{4}), (\frac{\pi}{2},-\frac{\pi}{8})$. (b) Performance of the code as function of the number of levels for different values of T_2 . (c) Accumulation of the error as a function of the number of "Logical Gate-Error Correction" cycles, for 6 qudit levels and $T_2 = 50~\mu s$, showing a linear trend as required for FT.

logical error is obtained by full state tomography of the logical state and corresponds to the failure probability of the EC procedure, i.e. to errors which cannot be corrected by the code. We immediately note that the slope of the curves in Fig. 3-(a) in log-log scale for the encoded LQ (number of levels ≥ 4) is larger than for the uncorrected case (blue line). This means that $\bar{\mathcal{E}}_e$ is propagated through the gadgets of the executed circuit to a higher order than the elementary error, thus demonstrating the Fault Tolerance of all the procedures involved.

Leakage errors could arise due to the finite duration of the pulses, but can be largely reduced by pulse-shaping techniques [55] and/or by using long pulses. Indeed, Figure 3-(a) shows that τ can be largely increased without compromising FT. For instance, by increasing τ by a factor 100 (dashed orange line), the slope of the curve for $T_2 \gtrsim 100~\mu s$ (still reasonable for several MNMs [56, 57]) does not change and hence the error is still propagated to a higher order compared to the uncorrected qubit. We only get a threshold in the minimal required T_2 .

Moreover, by increasing the LQ size d the error is further reduced and propagated to an even higher order, as evidenced by the increase of the slope of the curves in Fig. 3-(a). Remarkably, we find an almost exponential suppression of the error with a linear increase of d, as reported in Fig. 3-(b), independently of T_2 . The fi-

nal error suppression is strikingly large when compared to standard multi-qubit codes: here we achieve a logical error of 10^{-12} by employing 12×6 levels (LQ+ancilla) and $T_2 = 10 \mu s$, which should be compared to more than 5000 qubits needed by Floquet or surface codes with the same elementary error $p \approx \tau/T_2 = 3/1000$ [19]. This remarkable performance, obtained exploiting qudits with all-to-all connectivity, is here shown by focusing on the dominant family of errors of molecular qudits. The application of FTqd to other errors requires to identify suitable code words and will be focus of a future work. Moreover, the depth of our circuit does not increase with d, since all operations are implemented in parallel, again in contrast with standard codes. Finally, panel (c) shows the accumulation of the logical error after a sequence of gate-EC cycles. The perfectly linear trend shows that the procedure does not introduce any additional uncorrectable error, i.e. it is FT.

We now consider a two-qubit logical gate, such as the controlled-phase $C-\varphi$. This can be implemented by considering three interacting LQs, where the middle one acts as a switch of the effective coupling between the other two [58, 59], Q_1 and Q_2 (inset of Fig. 4). In presence of an interaction between the three units, excitations of the switch are dependent on the state of both Q_1 and Q_2 . This allows us to induce a 2π (semi-)resonant excitation of the switch (initialized in $|\bar{0}\rangle$) only for a specific $|\bar{\psi}_1\bar{\psi}_2\rangle$ logical state, such as $|\bar{1}1\rangle$. As a result, a phase is added only to the $|\bar{1}1\rangle$ component of the two-qubit log-

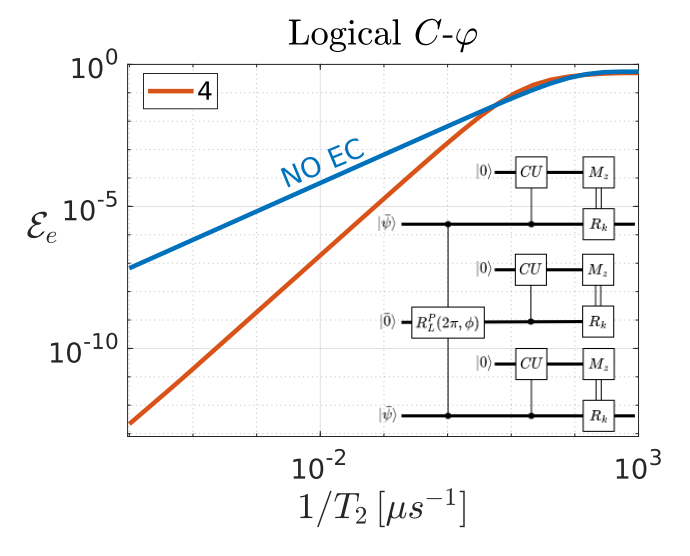


FIG. 4: Numerical simulation of the FT implementation of two-qubit logical gates. The uncorrectable logical error is shown as a function of $1/T_2$ at the end of a "Logical C- φ - EC" cycle. Simulations are computationally demanding and hence we limit to d=4. Inset: simulated circuit, with two logical qubits $|\bar{\psi}\rangle$ in a genric state, coupled by an error-corrected switch initialized in $|0_L\rangle$. Each unit is coupled to a d/2-levels ancilla for stabilization.

ical state [58–61], i.e. a $C-\varphi$ gate is implemented (see also SM). Since this involves a logical rotation $R_L^P(2\pi,0)$ of the switch, the latter must also be encoded and corrected. Simulation of the two-qubit gate followed by EC on all the three units is shown in Fig. 4 for d=4. As for single-qubit gates, the logical error is suppressed (here for $T_2\gtrsim 30~\mu {\rm s}$), thus demonstrating FTQC on a universal set of gates.

The scheme can be implemented also with simpler systems at the cost of reduced performance. For instance, single-spin molecules in presence of transverse magnetic fields and/or high-rank zero-field splitting anisotropy provide the all-to-all connectivity required by FTqd. Moreover, the scheme could be adapted to other multilevel quantum systems like impurity nuclear spins in semiconductor [48], atoms [62] or ion traps [45].

Conclusions – We have introduced a scheme for fault-tolerant quantum computing where each elementary logical qubit is encoded into a single multi-level qudit. The scheme only relies on an all-to-all connectivity between the state entering the definition of the logical qubit. The remarkable performance of the code is demonstrated by considering its implementation on a molecular spin architecture [61]. Our approach prevents the blowing up in the number of physical units, while yielding a large error suppression already with a small number of qudit levels, thus making the proposed route very appealing for an actual implementation.

[†]These Authors contributed equally to the work.

We warmly thank P. Santini for useful and stimulating discussions.

This work received financial support from European Union – NextGenerationEU, PNRR MUR project PE00000023-NQSTI, from the European Union's Horizon 2020 program under Grant Agreement No. 862893 (FET-OPEN project FATMOLS) and from Fondazione Cariparma. Project funded by the European Union – NextGenerationEU under the National Recovery and Resilience Plan (NRRP), Mission 4 Component 1 Investment 3.4 and 4.1.

- * stefano.carretta@unipr.it
- [1] R. Chao and B. W. Reichardt, Fault-tolerant quantum computation with few qubits, npj Quantum Inf. 4, 42 (2018).
- [2] D. Gottesman, An introduction to quantum error correction (2000), arXiv:quant-ph/0004072 [quant-ph].
- [3] S. J. Devitt, W. J. Munro, and K. Nemoto, Quantum error correction for beginners, Rep. Progr. Phys. 76, 076001 (2013).
- [4] D. Nigg, M. Müller, E. A. Martinez, P. Schindler, M. Hennrich, T. Monz, M. A. Martin-Delgado, and

- R. Blatt, Quantum computations on a topologically encoded qubit, Science **345**, 302 (2014).
- [5] B. M. Terhal, Quantum error correction for quantum memories, Rev. Mod. Phys. 87, 307 (2015).
- [6] E. Campbell, B. Terhal, and C. Vuillot, Roads towards fault-tolerant universal quantum computation, Nature 549, 172 (2017).
- [7] M. A. Nielsen and I. L. Chuang, Quantum Computation and Quantum Information (Cambridge university press, 2000).
- [8] P. Aliferis, D. Gottesman, and J. Preskill, Quantum accuracy threshold for concatenated distance-3 codes, Quant. Inf. Comput. 6, 97–165 (2006).
- [9] E. Knill, Quantum computing with realistically noisy devices, Nature 434, 39 (2005).
- [10] A. W. Cross, D. P. Divincenzo, and B. M. Terhal, A comparative code study for quantum fault tolerance, Quantum Info. Comput. 9, 541–572 (2009).
- [11] D. S. Wang, A. G. Fowler, and L. C. L. Hollenberg, Surface code quantum computing with error rates over 1%, Phys. Rev. A 83, 020302 (2011).
- [12] A. G. Fowler, A. M. Stephens, and P. Groszkowski, Highthreshold universal quantum computation on the surface code, Phys. Rev. A 80, 052312 (2009).
- [13] A. G. Fowler, M. Mariantoni, J. M. Martinis, and A. N. Cleland, Surface codes: Towards practical large-scale quantum computation, Phys. Rev. A 86, 032324 (2012).
- [14] A. M. Stephens, Fault-tolerant thresholds for quantum error correction with the surface code, Phys. Rev. A 89, 022321 (2014).
- [15] C. Chamberland, T. Jochym-O'Connor, and R. Laflamme, Thresholds for universal concatenated quantum codes, Phys. Rev. Lett. 117, 010501 (2016).
- [16] J. Marks, T. Jochym-O'Connor, and V. Gheorghiu, Comparison of memory thresholds for planar qudit geometries, New J. Phys. 19, 113022 (2017).
- [17] E. T. Campbell, Enhanced fault-tolerant quantum computing in d-level systems, Phys. Rev. Lett. 113, 230501 (2014).
- [18] M. Suchara, J. Kubiatowicz, A. Faruque, F. T. Chong, C.-Y. Lai, and G. Paz, Qure: The quantum resource estimator toolbox, in 2013 IEEE 31st International Conference on Computer Design (ICCD) (2013) pp. 419–426.
- [19] A. Paetznick, C. Knapp, N. Delfosse, B. Bauer, J. Haah, M. B. Hastings, and M. P. da Silva, Performance of planar floquet codes with majorana-based qubits, PRX Quantum 4, 010310 (2023).
- [20] E. Knill, R. Laflamme, R. Martinez, and C. Negrevergne, Benchmarking quantum computers: The five-qubit error correcting code, Phys. Rev. Lett. 86, 5811 (2001).
- [21] S. Pirandola, S. Mancini, S. L. Braunstein, and D. Vitali, Minimal qudit code for a qubit in the phase-damping channel, Phys. Rev. A 77, 032309 (2008).
- [22] A. Chiesa, E. Macaluso, F. Petiziol, S. Wimberger, P. Santini, and S. Carretta, Molecular nanomagnets as qubits with embedded quantum-error correction, J. Phys. Chem. Lett. 11, 8610 (2020).
- [23] M. H. Michael, M. Silveri, R. Brierley, V. V. Albert, J. Salmilehto, L. Jiang, and S. M. Girvin, New class of quantum error-correcting codes for a bosonic mode, Phys. Rev. X 6, 031006 (2016).
- [24] W. Cai, Y. Ma, W. Wang, C.-L. Zou, and L. Sun, Bosonic quantum error correction codes in superconducting quantum circuits, Fundamental Research 1, 50 (2021).

- [25] F. Petiziol, A. Chiesa, S. Wimberger, P. Santini, and S. Carretta, Counteracting dephasing in molecular nanomagnets by optimized qudit encodings, npj Quantum Inf. 7, 133 (2021).
- [26] S. Carretta, D. Zueco, A. Chiesa, A. Gómez-León, and F. Luis, A perspective on scaling up quantum computation with molecular spins, Appl. Phys. Lett. 118, 240501 (2021).
- [27] M. Chizzini, L. Crippa, L. Zaccardi, E. Macaluso, S. Carretta, A. Chiesa, and P. Santini, Quantum error correction with molecular spin qudits, Phys. Chem. Chem. Phys. 24, 20030 (2022).
- [28] P. Reinhold, S. Rosenblum, W.-L. Ma, L. Frunzio, L. Jiang, and R. J. Schoelkopf, Error-corrected gates on an encoded qubit, Nat. Phys. 16, 822 (2020).
- [29] S. Puri, L. St-Jean, J. A. Gross, A. Grimm, N. E. Frattini, P. S. Iyer, A. Krishna, S. Touzard, L. Jiang, A. Blais, S. T. Flammia, and S. M. Girvin, Bias-preserving gates with stabilized cat qubits, Sci. Adv. 6, eaay5901 (2020).
- [30] S. Rosenblum, P. Reinhold, M. Mirrahimi, L. Jiang, L. Frunzio, and R. J. Schoelkopf, Fault-tolerant detection of a quantum error, Science 361, 266 (2018).
- [31] L. Hu, Y. Ma, W. Cai, X. Mu, Y. Xua, W. Wang, Y. Wu, H. Wang, Y. P. Song, C.-L. Zou, S. M. Girvin, L.-M. Duan, and L. Sun, Quantum error correction and universal gate set operation on a binomial bosonic logical qubit, Nat. Phys. 15, 503–508 (2019).
- [32] A. Chiesa, F. Petiziol, M. Chizzini, P. Santini, and S. Carretta, Theoretical design of optimal molecular qudits for quantum error correction, J. Phys. Chem. Lett. 13, 6468 (2022).
- [33] E. Knill and R. Laflamme, Theory of quantum errorcorrecting codes, Phys. Rev. A 55, 900 (1997).
- [34] Y. Ma, Y. Xu, X. Mu, W. Cai, L. Hu, W. Wang, X. Pan, H. Wang, Y. P. Song, C.-L. Zou, and L. Sun, Errortransparent operations on a logical qubit protected by quantum error correction, Nat. Phys. 16, 827–831 (2020).
- [35] A. G. Fowler, A. C. Whiteside, and L. C. L. Hollenberg, Towards practical classical processing for the surface code, Phys. Rev. Lett. 108, 180501 (2012).
- [36] S. Bravyi, M. Suchara, and A. Vargo, Efficient algorithms for maximum likelihood decoding in the surface code, Phys. Rev. A 90, 032326 (2014).
- [37] The relative phase between $|\ell,k\rangle|0\rangle$ and $|\ell,k\rangle|k\rangle$ is necessary to ensure that the corresponding Hamiltonian has zero diagonal. Since the ancilla is initialized in $|0\rangle$, this relative phase is irrelevant.
- [38] D. Gatteschi, R. Sessoli, and J. Villain, Molecular Nanomagnets (Oxford University Press, 2006).
- [39] M. Shiddiq, D. Komijani, Y. Duan, A. Gaita-Ariño, E. Coronado, and S. Hill, Enhancing coherence in molecular spin qubits via atomic clock transitions., Nature 531, 348 (2016).
- [40] F. Troiani and M. G. A. Paris, Universal quantum magnetometry with spin states at equilibrium, Phys. Rev. Lett. 120, 260503 (2018).
- [41] A. Gaita-Ariño, F. Luis, S. Hill, and E. Coronado, Molecular spins for quantum computation., Nat. Chem. 11, 301 (2019).
- [42] M. Atzori and R. Sessoli, The second quantum revolution: Role and challenges of molecular chemistry, J. Am. Chem. Soc. 141, 11339 (2019).
- [43] M. Chizzini, L. Crippa, A. Chiesa, F. Tacchino, F. Petiziol, I. Tavernelli, P. Santini, and S. Carretta, Molecu-

- lar nanomagnets with competing interactions as optimal units for qudit-based quantum computation, Phys. Rev. Res. 4, 043135 (2022).
- [44] C. D. Bruzewicz, J. Chiaverini, R. McConnell, and J. M. Sage, Trapped-ion quantum computing: Progress and challenges, Appl. Phys. Lett. 6, 021314 (2019).
- [45] M. Ringbauer, M. Meth, L. Postler, R. Stricker, R. Blatt, P. Schindler, and T. Monz, A universal qudit quantum processor with trapped ions, Nat. Phys. 18, 1053–1057 (2022).
- [46] S. Kuhr, W. Alt, D. Schrader, I. Dotsenko, Y. Miroshnychenko, A. Rauschenbeutel, and D. Meschede, Analysis of dephasing mechanisms in a standing-wave dipole trap, Phys. Rev. A 72, 023406 (2005).
- [47] A. Morello, J. J. Pla, P. Bertet, and D. N. Jamieson, Donor spins in silicon for quantum technologies, Adv. Quantum Technol. 3, 2000005 (2020).
- [48] A. Chatterjee, P. Stevenson, S. De Franceschi, A. Morello, N. P. de Leon, and F. Kuemmeth, Semiconductor qubits in practice, Nat. Rev. Phys. 3, 157 (2021).
- [49] M. Fataftah, J. M. Zadrozny, S. C. Coste, M. J. Graham, D. M. Rogers, and D. E. Freedman, Employing forbidden transitions as qubits in a nuclear spin-free chromium complex., J. Am. Chem. Soc. 138, 1344 (2016).
- [50] K. Bader, M. Winkler, and J. van Slageren, Tuning of molecular qubits: Very long coherence and spin–lattice relaxation times, Chem. Commun., 3623 (2016).
- [51] Y.-S. Ding, Y.-F. Deng, and Y.-Z. Zheng, The rise of single-ion magnets as spin qubits, Magnetochem. 2, 40 (2016).
- [52] M. N. Leuenberger and D. Loss, Grover algorithm for large nuclear spins in semiconductors, Phys. Rev. B 68, 165317 (2003).
- [53] This is due to the specific form of the error words $\{|\ell, k\rangle\}$, in which differ the two $\ell = 0, 1$ subspaces are disjoint for all k.
- [54] \mathcal{F}_e is the average fidelity on the initial states $|0_L\rangle$, $|1_L\rangle$, $\frac{1}{\sqrt{2}}(|0\rangle + |1\rangle)$, $\frac{1}{\sqrt{2}}(|0\rangle |1\rangle)$, $\frac{1}{\sqrt{2}}(|0\rangle + i|1\rangle)$, $\frac{1}{\sqrt{2}}(|0\rangle i|1\rangle)$. [55] A. Castro, A. García Carrizo, S. Roca, D. Zueco, and
- [55] Å. Castro, A. García Carrizo, S. Roca, D. Zueco, and F. Luis, Optimal control of molecular spin qudits, Phys. Rev. Appl. 17, 064028 (2022).
- [56] K. Bader, D. Dengler, S. Lenz, B. Endeward, S.-D. Jiang, P. Neugebauer, and J. van Slageren, Room temperature quantum coherence in a potential molecular qubit, Nat. Comm. 5, 5304 (2014).
- [57] J. M. Zadrozny, J. Niklas, O. G. Poluektov, and D. E. Freedman, Millisecond coherence time in a tunable molecular electronic spin qubit., ACS Cent. Sci. 1, 488 (2015)
- [58] J. Ferrando-Soria, E. Moreno-Pineda, A. Chiesa, A. Fernandez, S. A. Magee, S. Carretta, P. Santini, I. Vitorica-Yrezabal, F. Tuna, E. J. L. McInness, and R. E. P. Winpenny, A modular design of molecular qubits to implement universal quantum gates., Nat. Commun. 7, 11377 (2016).
- [59] A. Chiesa, F. Petiziol, E. Macaluso, S. Wimberger, P. Santini, and S. Carretta, Embedded quantum-error correction and controlled-phase gate for molecular spin qubits, AIP Adv. 11, 025134 (2021).
- [60] A. Chiesa, G. F. S. Whitehead, S. Carretta, L. Carthy, G. A. Timco, S. J. Teat, G. Amoretti, E. Pavarini, R. E. P. Winpenny, and P. Santini, Molecular nanomagnets with switchable coupling for quantum simulation.,

- Sci. Rep. 4, 7423 (2014).
- [61] A. Chiesa, S. Roca, S. Chicco, M. de Ory, A. Gómez-León, A. Gomez, D. Zueco, F. Luis, and S. Carretta, Blueprint for a molecular-spin quantum processor, Phys.
- Rev. Appl. 19, 064060 (2023).
- [62] A. V. Gorshkov, M. Hermele, V. Gurarie, C. Xu, P. S. Julienne, J. Ye, P. Zoller, E. Demler, M. D. Lukin, and A. M. Rey, Two-orbital s u(n) magnetism with ultracold alkaline-earth atoms, Nat. Phys. 6, 289 (2010).